Electronic Supplementary Material (ESI) for Analytical Methods.

Supplementary Information

Chelation Therapy-inspired Design of a Water-stable Fluorescent Probe for Effectual Monitoring of Copper(II) ions in Real Water

Suvojit Roy,[a] Prosenjit Choudhury,[b] and Bhaskar Biswas[a,*]

[a]*Department of Chemistry, University of North Bengal, Darjeeling 734013, India.*

[b]*Department of Physics, Dr. Meghnad Saha College, Itahar, Uttar Dinajpur 733128, India.*

Table of Content

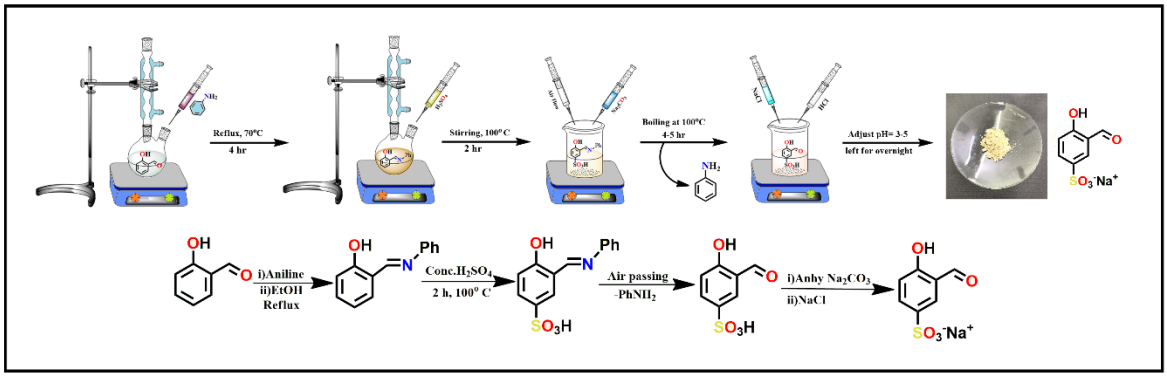

Scheme S1. Synthesis of the precursor, sodium salt of salicylaldehyde-5-sulphonate.

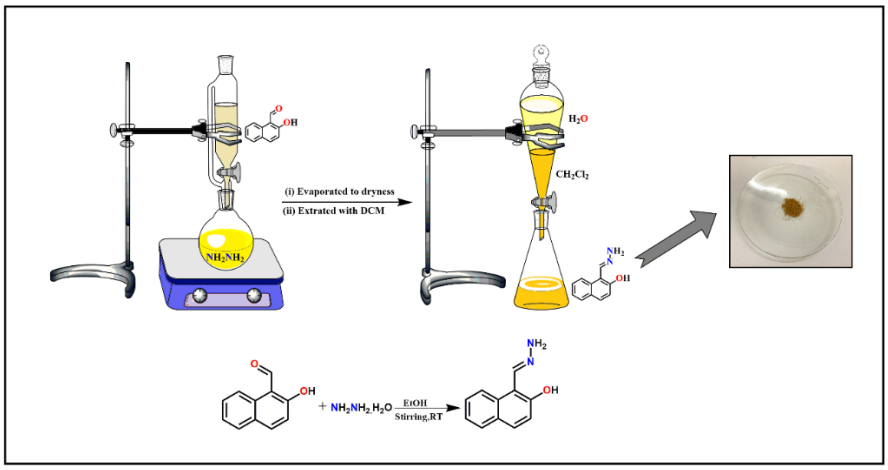

Scheme S2. Synthesis of the precursor, 2-hydroxy naphthalene hydrazone.

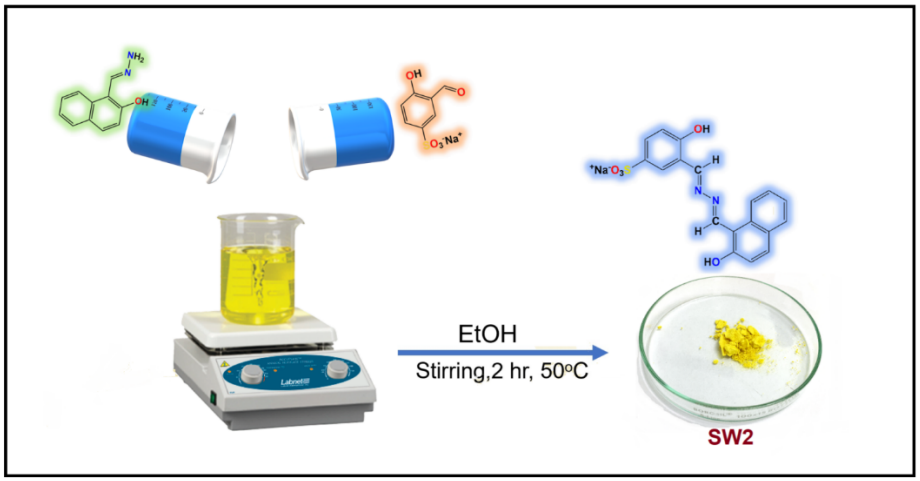

Scheme S3. Synthesis of the Chemosensor, **SW2**.

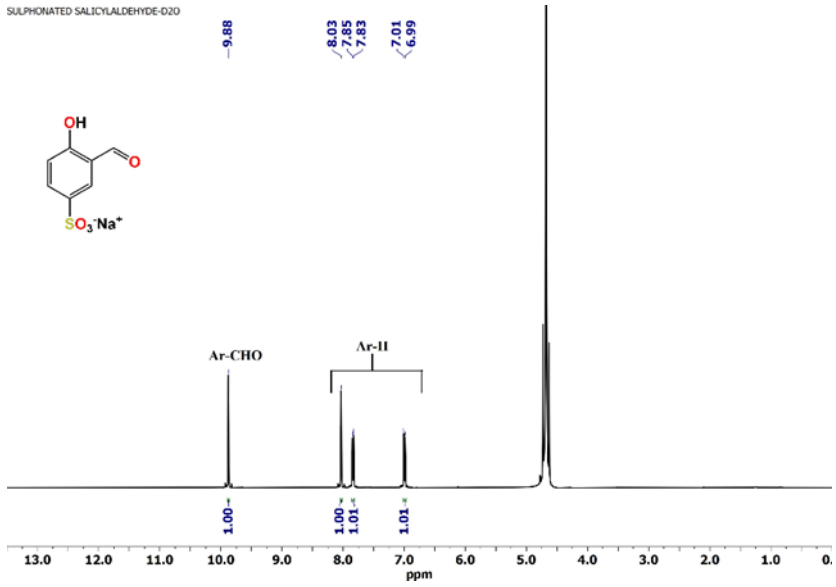

Fig. S1. ^{1}H NMR spectrum (400 MHz, D_2O) of the precursor, sodium salt of salicyldehyde-5-sulphonate.

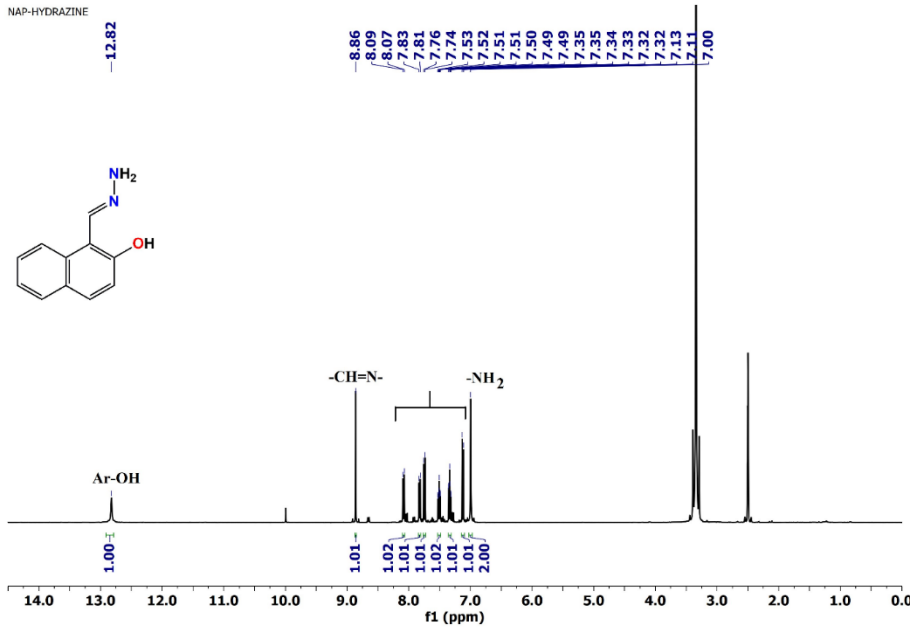

Fig. S2. ^{1}H NMR spectrum (400 MHz, DMSO-d^6) of the precursor, 2-hydroxy naphthalene hydrazone.

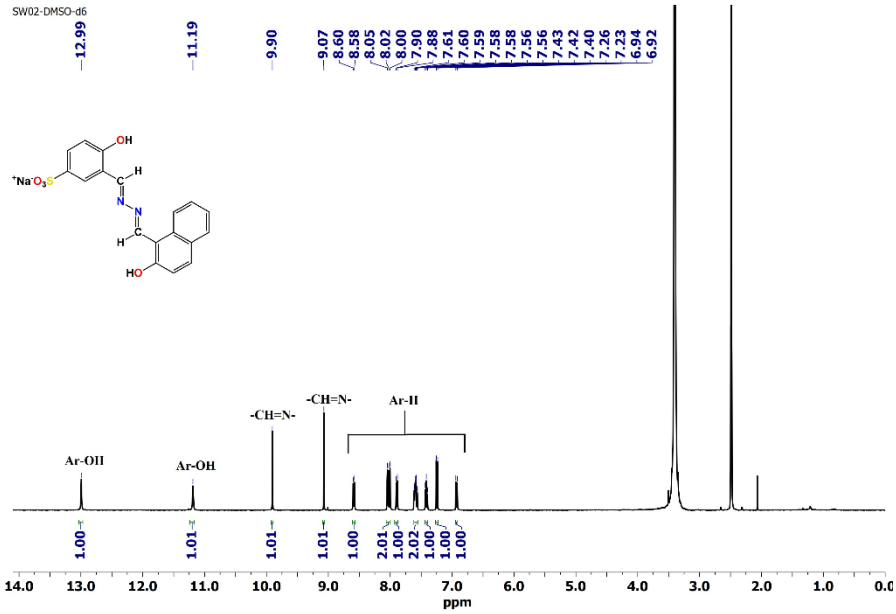

Fig. S3. ^{1}H NMR spectrum (400 MHz, DMSO-d^{6}) of **SW2**.

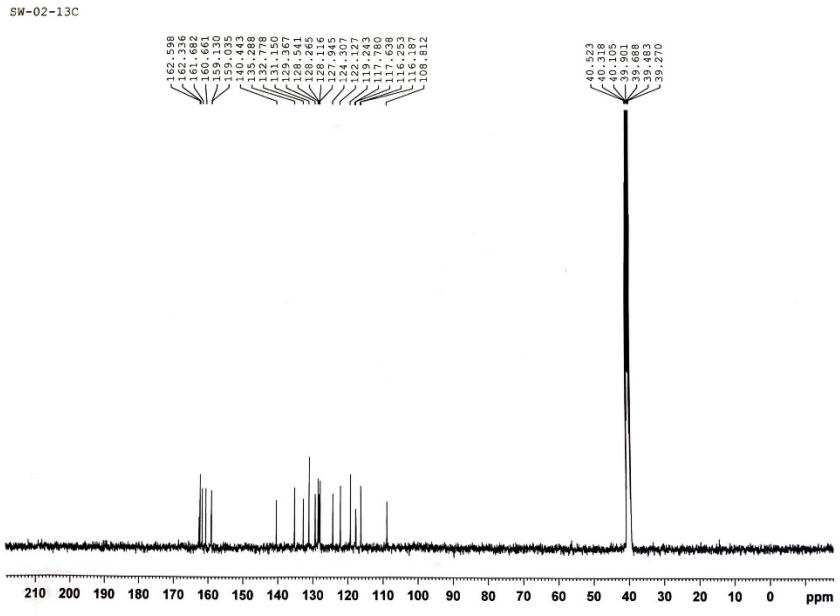

Fig. S4. ^{13}C NMR spectrum (101 MHz, DMSO-d^{6}) of **SW2**.

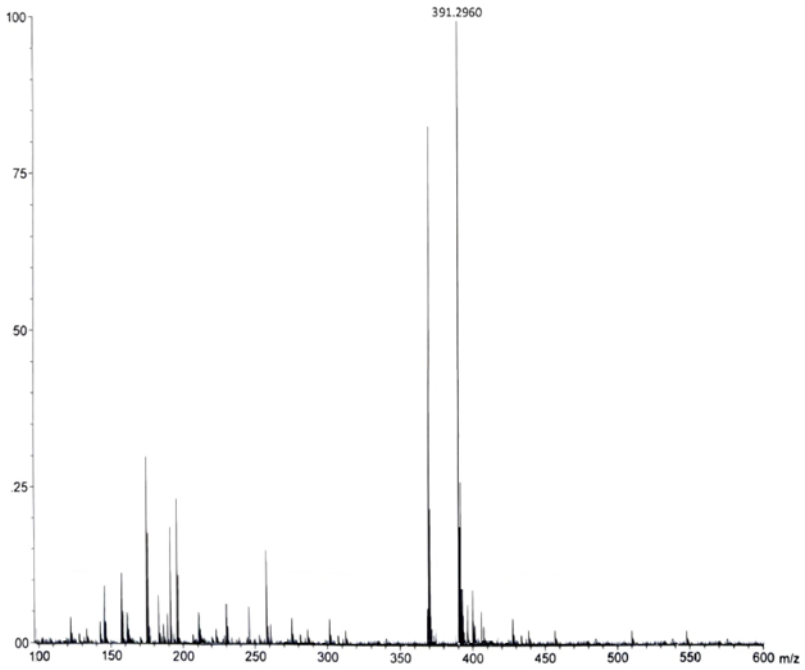

Fig. S5. ESI-MS of **SW2** in water.

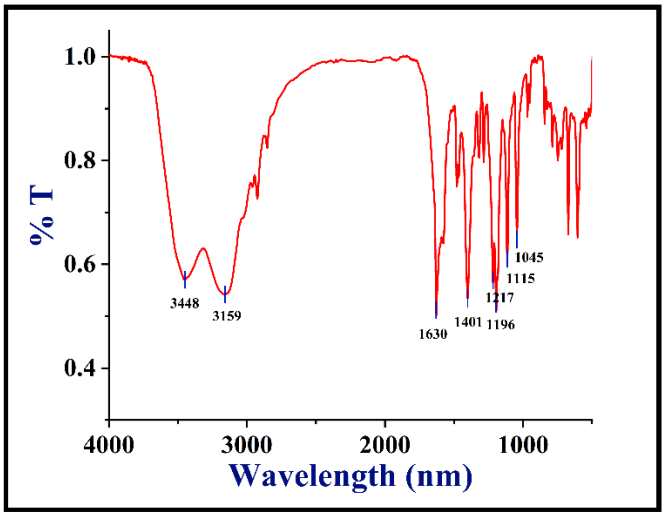

Fig. S6. FT-IR spectrum of the chemosensor, **SW2**.

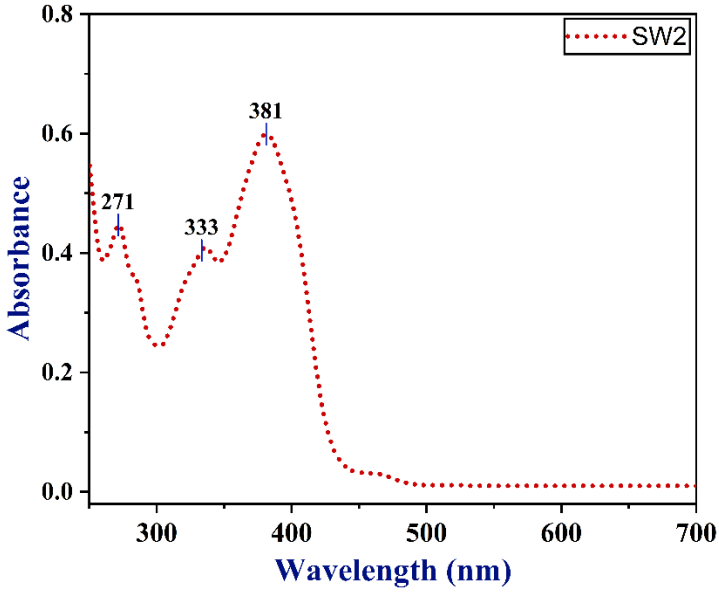

Fig. S7. UV-Vis spectrum of the chemosensor, **SW2.**

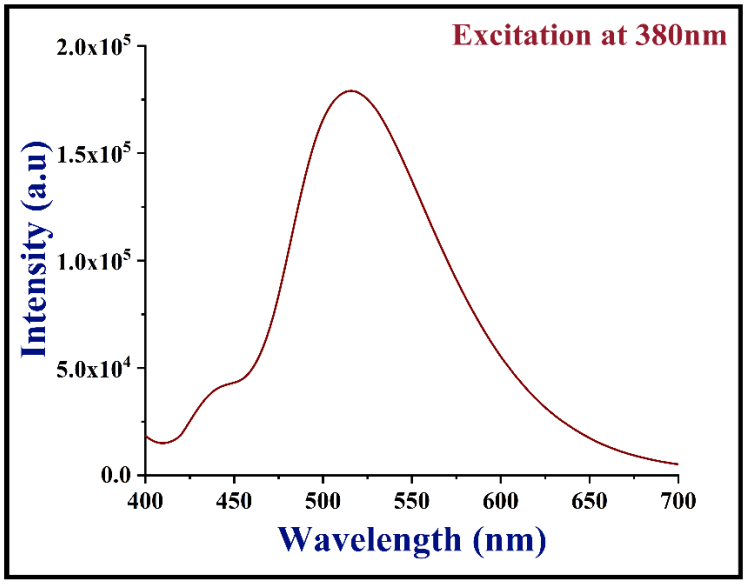

Fig. S8. Fluorescence spectra of **SW2** in water.

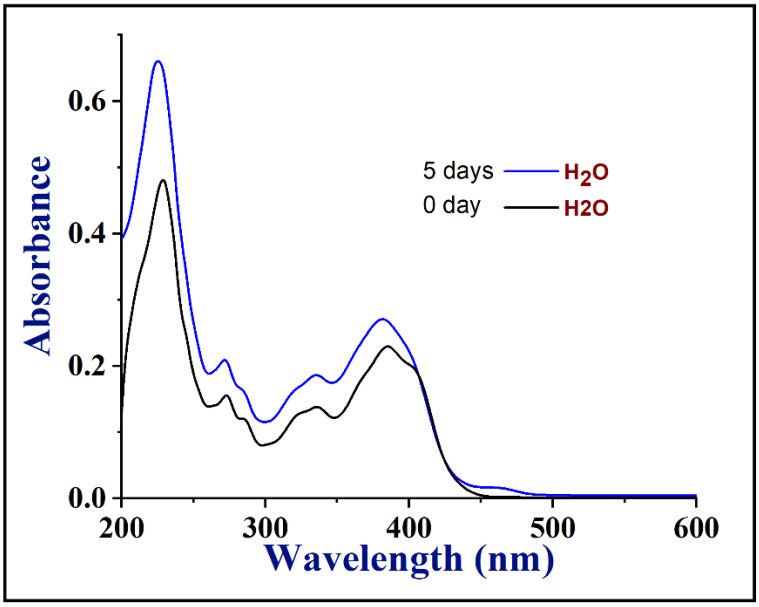

Fig. S9. Water-phase stability of **SW2** for 5 days.

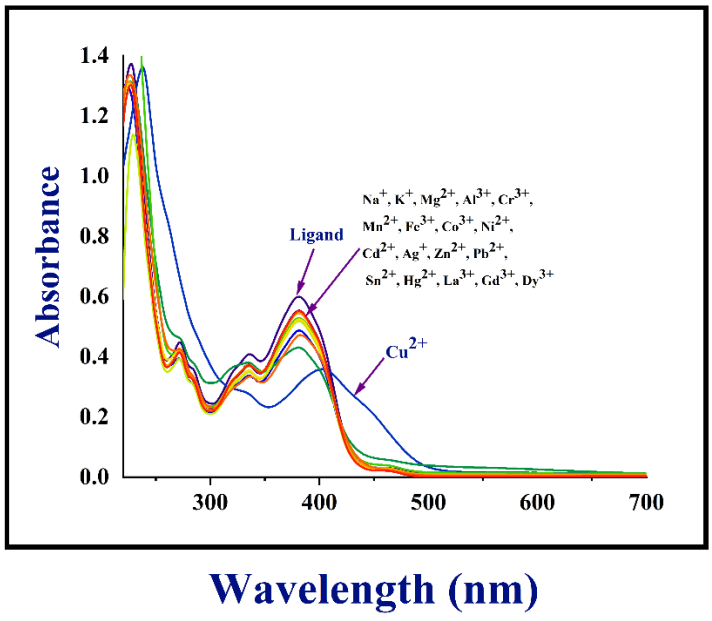

Fig. S10. Spectrophotometry study of **SW2** with Cu (II) and other metal ions ($M^{+/2+/3+}$) in H_2O medium at 298 K.

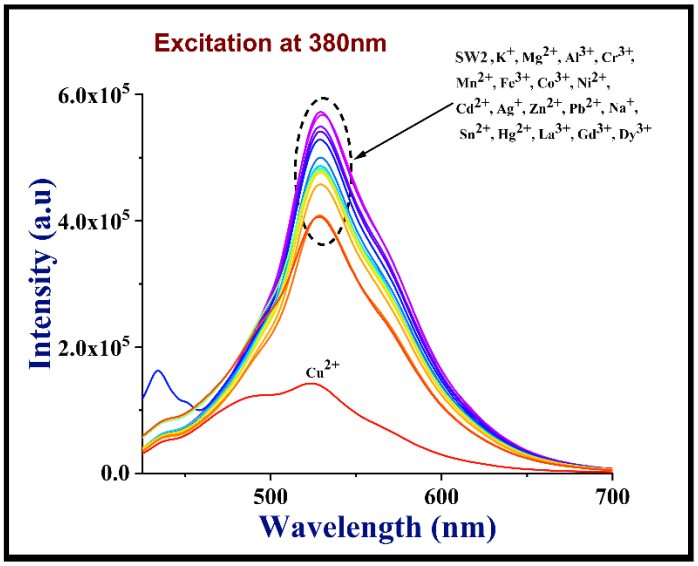

Fig. S11. Spectrofluorimetric study of **SW2** with Cu (II) and other metal ions ($M^{+/2+/3+}$) in H_2O medium at 298 K.

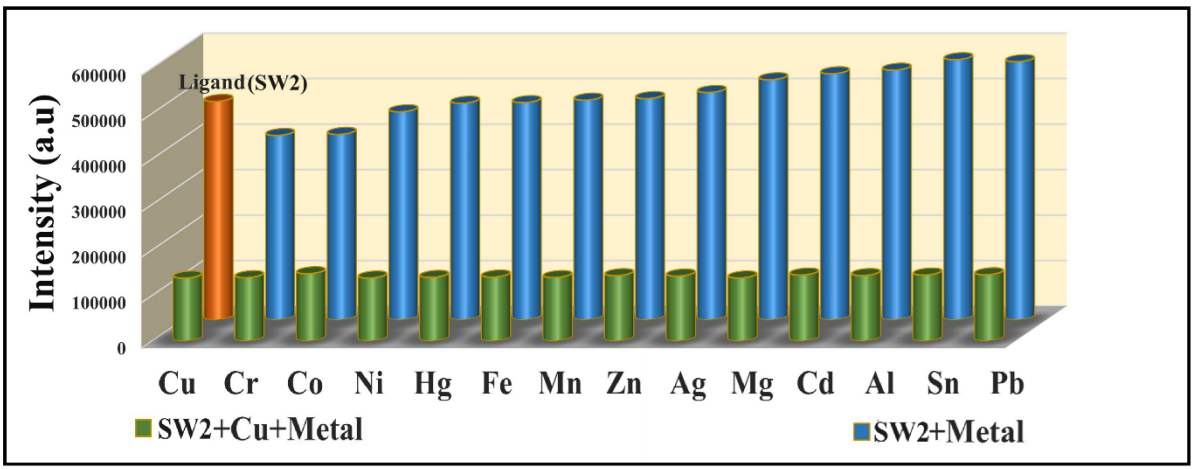

Fig. S12. Fluorescence response of **SW2** towards Cu^{2+} ions coexistence of other metal ions in aqueous medium.

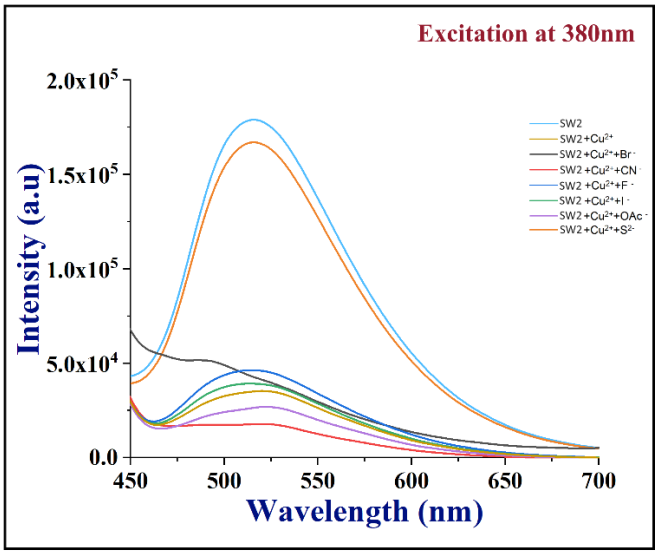

Fig. S13. Fluorescence spectra of **SW2** towards Cu^{2+} in presence of different anions.

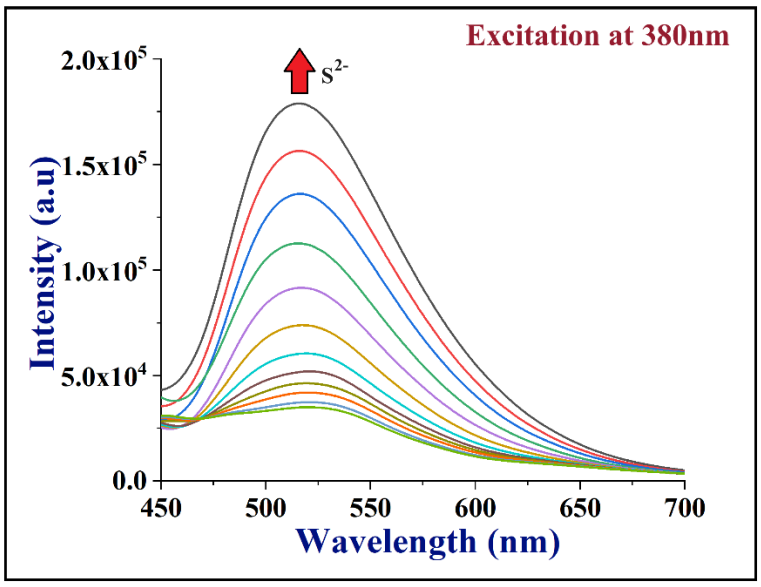

Fig. S14. Changes in the fluorescence spectrum upon a gradual addition of S^{2-} to **SW2-Cu^{2+}** complex in H_2O.

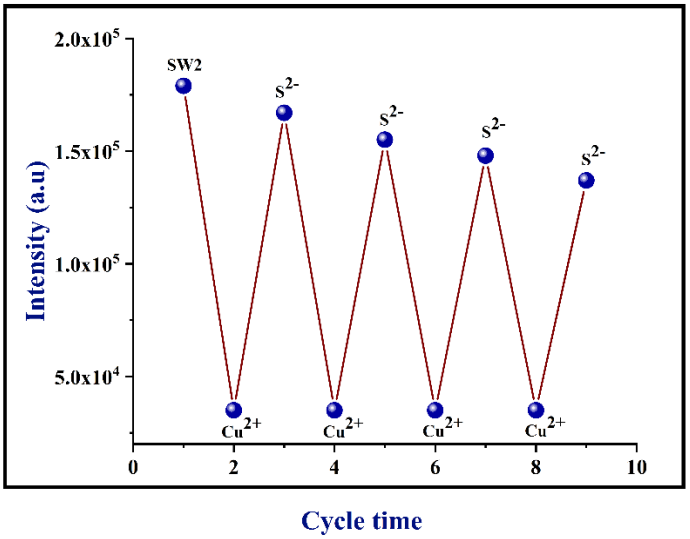

Fig. S15. Reversible switching cycles of fluorescence by alternating adding Cu^{2+} and S^{2-}.

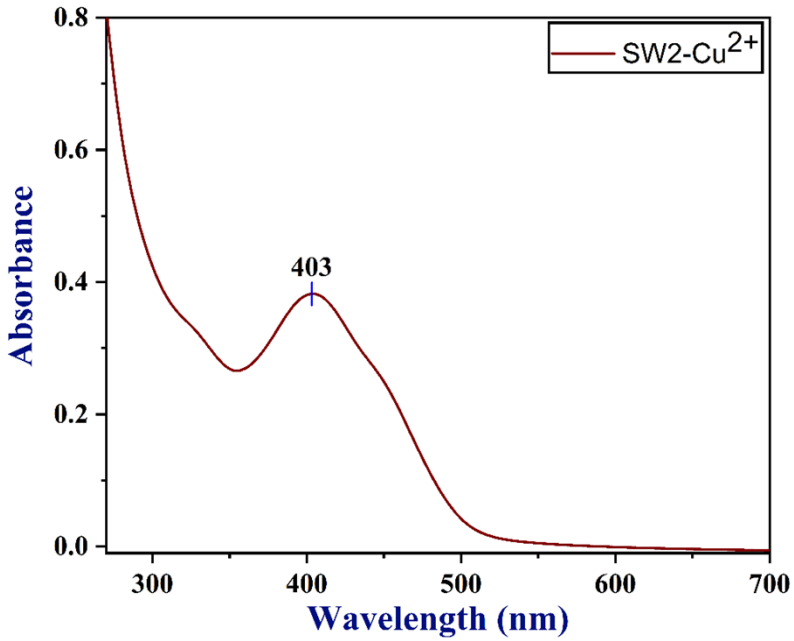

Fig. S16. UV-Vis spectrum of the **SW2-Cu^{2+} complex**.

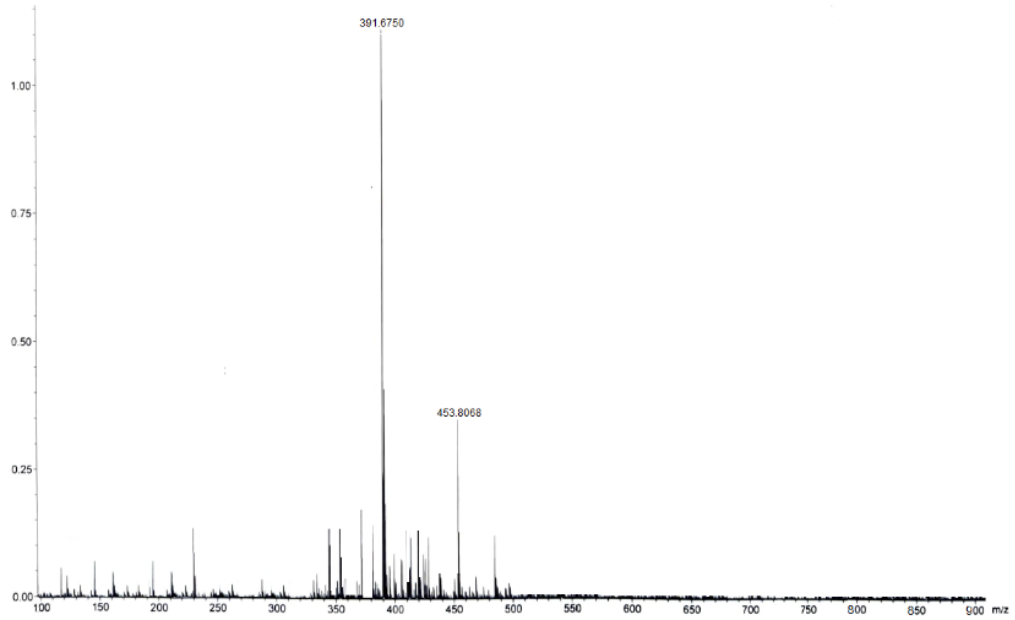

Fig. S17. ESI-MS of the **SW2-Cu^{2+} complex**.

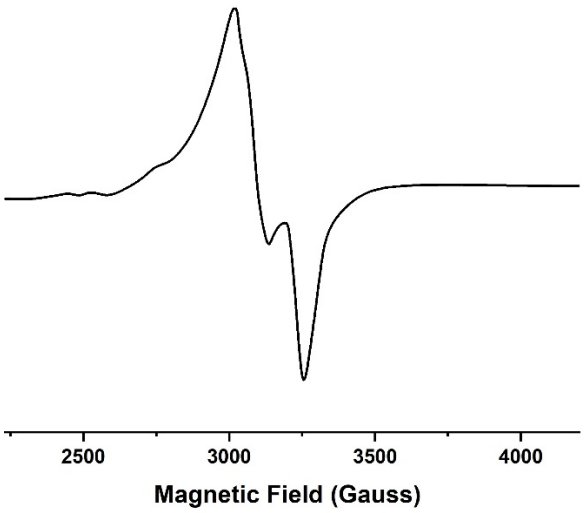

Fig. S18. EPR of the **SW2-Cu^{2+} complex**.

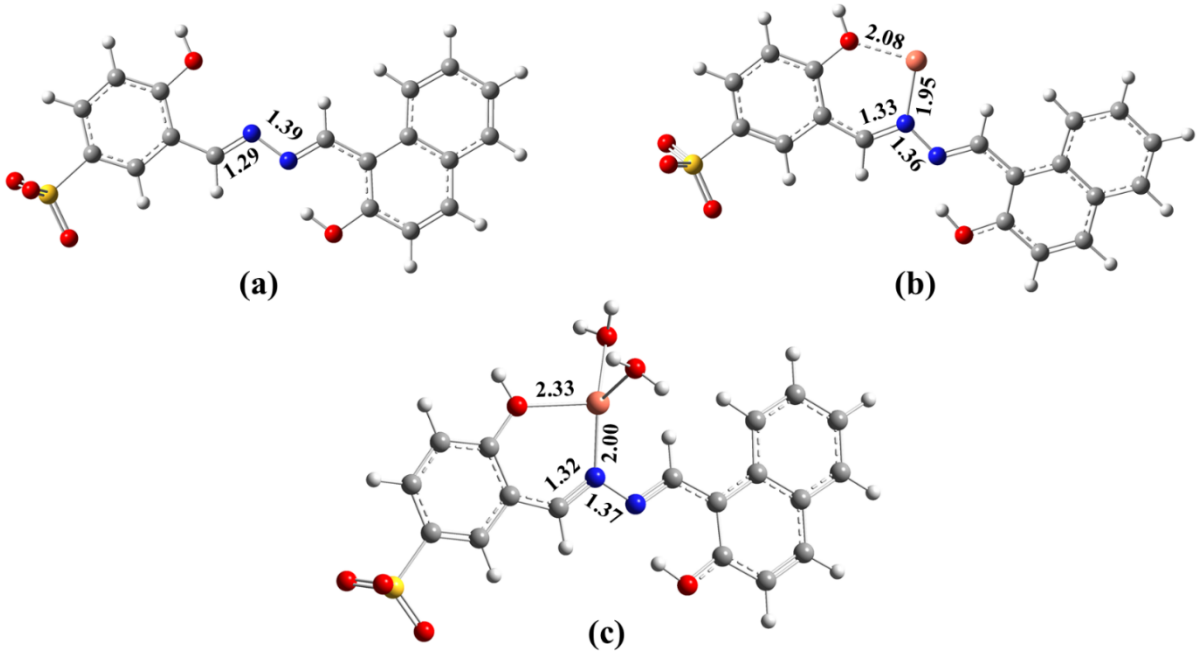

Fig. S19. Ground state optimized geometries of the (a) **SW2** (b) **SW2-Cu^{2+}** (c) **SW2-Cu^{2+} aqua complex**.

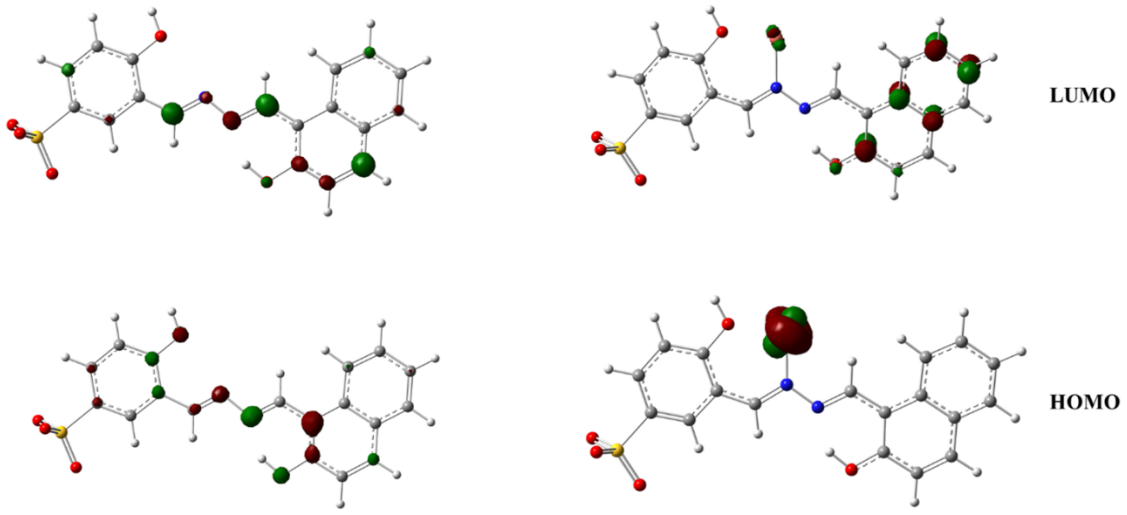

Fig.S20. The electron cloud distribution of LUMO and HOMO orbitals of **SW2** and **SW2-Cu^{2+}.**

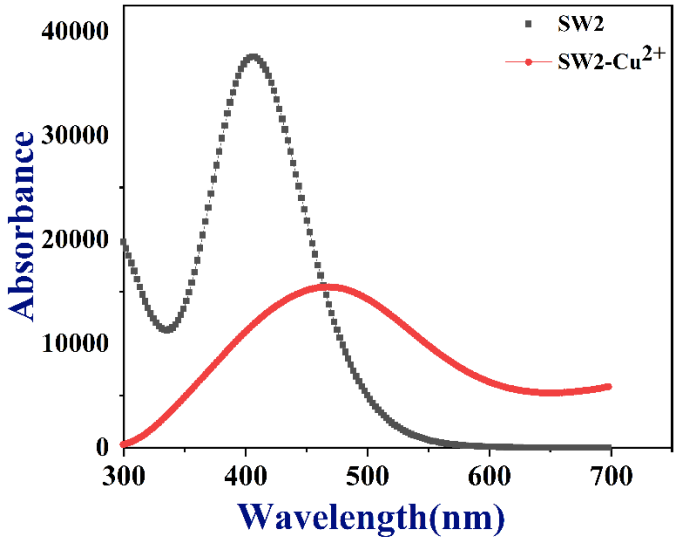

Fig. S21. Theoretical adsorption spectra of **SW2** and **SW2-Cu^{2+}**.

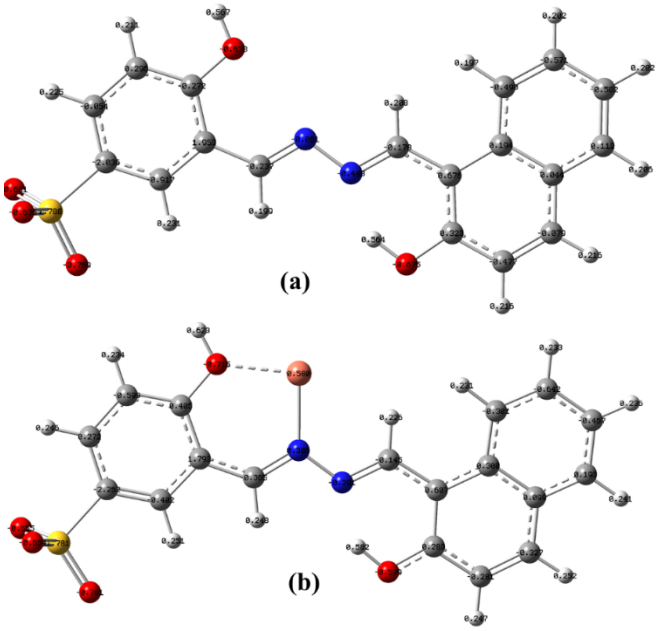

Fig. S22. Mulliken charge analysis of the (a) **SW2** (b) **SW2-Cu^{2+}**.

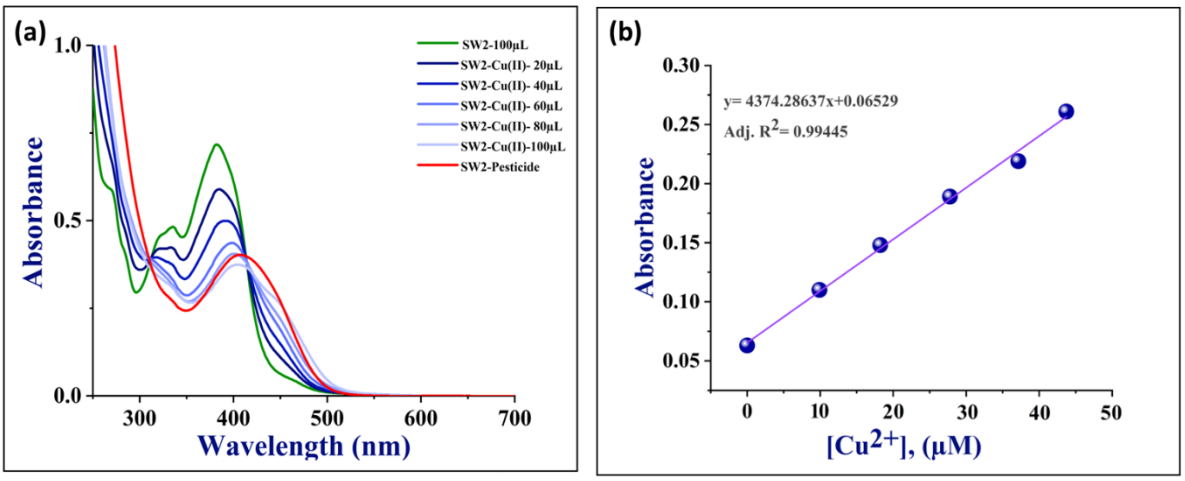

Fig. S23. (a) Spectrophotometric analysis for the determination of the concentration of Cu^{2+} ion in the pesticide-contaminated water by comparing a known concentration of $CuCl_2$; (b) Determination of the concentration of Cu^{2+} ion in the pesticide-contaminated water.

Table S1: Computed absorption wavelengths (λ_{max} in nm), vertical excitation energies (E_{0-0} in eV), oscillator strengths (f), the composition of the corresponding electronic transitions (H, HOMO; L, LUMO) of **SW2** calculated by using B3LYP/6–31+G(d) level of theory.

No. of States	λ_{max}**(nm)**	$E_{0-0}(eV)$	**Oscillator Strength (** f**)**	**Major contributions**
1	406.96	3.05	0.919	HOMO->LUMO (99%)
2	350.09	3.54	0.0002	H-4->LUMO (98%)
3	337.77	3.67	0.0679	H-1->LUMO (92%)
4	329.17	3.77	0.0783	H-2->LUMO (90%)
5	309.09	4.01	0.0012	HOMO->L+1 (85%)
6	306.50	4.04	0.0001	H-3->LUMO (97%)
7	292.57	4.24	0.4236	H-5->LUMO (83%)
8	273.32	4.54	0.0496	HOMO->L+2 (31%)
9	269.68	4.60	0.0291	HOMO->L+2 (57%)
10	266.36	4.65	0.0309	HOMO->L+3 (38%)
11	262.53	4.72	0.0001	H-4->L+1 (88%)
12	255.80	4.85	0.1035	HOMO->L+3 (45%)
13	246.78	5.02	0.0023	H-7->LUMO (53%)
14	246.36	5.03	0.0124	H-6->LUMO (65%)
15	244.40	5.07	0.0001	H-3->L+1 (95%)
16	243.54	5.09	0.0001	H-8->LUMO (68%)
17	239.82	5.17	0.4494	H-2->L+1 (42%)
18	237.39	5.22	0.0133	H-5->L+1 (52%)
19	235.71	5.26	0.0677	H-9->LUMO (57%)
20	231.06	5.37	0.001	H-1->L+2 (42%)
21	230.77	5.37	0	HOMO->L+5 (78%)
22	227.50	5.45	0.0005	H-3->L+3 (86%)
23	226.94	5.46	0.026	H-2->L+2 (35%)
24	226.03	5.49	0.0002	H-4->L+2 (85%)
25	224.11	5.53	0.0004	HOMO->L+7 (79%)
26	222.93	5.56	0.2583	H-1->L+3 (41%)
27	222.60	5.57	0.0023	HOMO->L+6 (77%)
28	219.42	5.65	0.167	H-2->L+4 (36%)
29	217.54	5.70	0.0001	H-4->L+3 (97%)
30	216.84	5.72	0.361	H-1->L+4 (52%)

Table S2: Computed absorption wavelengths (λ_{max} in nm), vertical excitation energies (E_{0-0} in eV), oscillator strengths (f), the composition of the corresponding electronic transitions (H, HOMO; L, LUMO) of **SW2-Cu^{2+}** Calculated by using B3LYP/6–31+G(d)/LAN2DZP level of theory.

No. of States	λ_{max}**(nm)**	$E_{0-0}(eV)$	**Oscillator Strength (**f**)**	**Major contributions**
1	1350.149113	0.918268944	0.0005	H-2(B)->LUMO(B) (70%)
2	1218.517867	1.017465589	0.0059	H-3(B)->LUMO(B) (90%)
3	1080.94327	1.14696121	0.024	HOMO(B)->LUMO(B) (90%)
4	1049.113158	1.181760033	0.1255	H-1(B)->LUMO(B) (59%)
5	831.717938	1.490649586	0.1349	H-4(B)->LUMO(B) (95%)
6	733.1137241	1.691142805	0.0001	H-5(B)->LUMO(B) (99%)
7	679.7379003	1.823938314	0.0001	H-6(B)->LUMO(B) (94%)
8	670.6198237	1.848737476	0	H-7(B)->LUMO(B) (99%)
9	629.2974978	1.97013337	0.0435	H-9(B)->LUMO(B) (89%)
10	560.3552066	2.212525172	0.0001	H-8(B)->LUMO(B) (99%)
11	544.6263695	2.276423011	0	H-10(B)->LUMO(B) (96%)
12	535.2682857	2.316221665	0.0061	H-11(B)->LUMO(B) (71%)
13	505.0272628	2.454916975	0.1906	HOMO(A)->LUMO(A) (61%)
14	488.5691493	2.537614178	0.0029	H-15(B)->LUMO(B) (84%)
15	475.2355131	2.60881177	0.0967	H-12(B)->LUMO(B) (63%)
16	447.8712315	2.768206379	0.0001	H-2(A)->LUMO(A) (90%)
17	446.2110164	2.778506031	0.0016	H-16(B)->LUMO(B) (46%)
18	428.6698925	2.892202186	0.1447	H-3(A)->LUMO(A) (30%)
19	420.8703385	2.945800373	0.0031	H-2(B)->L+1(B) (70%)
20	406.7989796	3.047696927	0.0039	H-1(A)->LUMO(A) (88%)
21	402.9254591	3.076995936	0.0252	H-4(B)->L+1(B) (18%)
22	391.8837885	3.163693004	0.0642	H-16(B)->LUMO(B) (26%)
23	385.8469269	3.21319133	0.0001	HOMO(B)->L+1(B) (96%)
24	384.7811837	3.222091029	0.0008	H-2(A)->L+2(A) (46%)
25	381.9128666	3.24629021	0.0016	H-13(B)->LUMO(B) (55%)
26	381.6777275	3.248290143	0.0016	H-14(B)->LUMO(B) (48%)
27	374.9937786	3.306188184	0.0087	H-3(A)->LUMO(A) (30%)
28	356.5120425	3.477582388	0.0458	H-17(B)->LUMO(B) (40%)
29	348.9759992	3.552679848	0	H-6(A)->LUMO(A) (95%)
30	343.446518	3.609877914	0.0238	HOMO(A)->L+1(A) (29%)